*Vietnam Journal of Science and Technology* ***56*** *(3B) (2018) 104-116*

# THE ROLE OF COUNTER ANIONS IN ANTICORROSIVE PROPERTIES OF SILICA-POLYPYRROLE COMPOSITE

**Vu Thi Hai Van[1, 2], Pham Thi Nam[1], Nguyen Thi Thom[1], Nguyen Thu Phuong[1], Nguyen Thi Thu Trang[1], To Thi Xuan Hang[1], Dinh Thi Mai Thanh[1, 3, *]**

[1]*Institute for Tropical Technology, VAST, 18 Hoang Quoc Viet, Cau Giay, Ha Noi*

[2]*Graduate University of Science and Technology, VAST, 18 Hoang Quoc Viet, Cau Giay District, Ha Noi*

[3]*University of Science and Technology of Hanoi, VAST, 18 Hoang Quoc Viet, Cau Giay District, Ha Noi*

[*]Email*: dmthanh@itt.vast.vn*

Received: 20 July 2018; Accepted for publication: 9 September 2018

## ABSTRACT

Silica/Polypyrrole ($SiO_2$/PPy) composites were synthesized in the presence of different counter anions as oxalate (Ox), benzoate (Bz) and dodecyl sulfate (DoS). The morphology and properties of composites were characterized by FTIR, EDX, SEM, TGA and CV method through the two-point-electrode. The synthesized composites were loaded in polyvinylbutyral (PVB) to develop coating for mild steel substrates. A comparative study of the corrosion protection efficiency of carbon steel coated with PVB and PVB containing composites was evaluated by measurement of open circuit potential (OCP), Tafel polarization and electrochemical impedance spectroscopy (EIS). It was found that $SiO_2$/PPyOx could provide much better protection, with the lowest current density ($4.81\times10^{-8}$ A.cm$^{-2}$ and highest impedance modulus ($6.25\times10^{-8}$ Ω.cm$^{-2}$) when compared with $SiO_2$/PPyDoS and $SiO_2$/PPyBz due to the small size and inhibitive ability of oxalate anion.

*Keywords:* silica/polypyrrole, counter anions, corrosion protection, PVB coating.

## 1. INTRODUCTION

The serious consequences of the corrosion process have become a global problem which cost US$2.5 trillion per year, equivalent to roughly 3.4 percent of the global Gross Domestic Product [1]. Generally, the common way to protect or reduce the corrosion rate is coating on the metals or alloys surface. Chromate coatings showed anticorrosion abilities in many aggressive environments, however, it is extremely toxic and contemplated as an environment pollutant [2].

Corrosion protection by organic coating is brought about by barrier effect and internal sacrificial electrode formation, protecting the underlying metal from further corrosion. Conventional polymer coating as polyvinyl butyral (PVB) is well known due to its superior characteristics, good scratch resistance and adhesion to metal surface [3]. In general, it is

reported that the additional of suitable reinforcing filler not only improve the adhesion strength between polymer and metal surface but also increase the diffusion paths of water and oxygen molecules through the coating, thus enhancing the corrosion resistance of the coating [4].

There are clear evidences that nanoparticles in polymer coating can increase the mechanical, thermal properties and corrosion resistance of the coating [5]. Nano silica is a potential candidate among the inorganic oxides in terms of high surface area, good dispersion, low cost and high efficiency [6]. Recently, organic/inorganic coating composites is received attentions from industrial and academic interests. The inorganic fillers can significantly enhance thermal stability and mechanical properties of polymers when organic compound with unusual characteristics can be used for several applications [7].

Conducting polymers have become a new field of materials to be explored since the discovery of Heeger, Shirakawa and MacDiarmid in the late of 70's [8-10]. Among these conducting polymers, Polypyrrole (PPy) is a promising candidate due to its friendly environmental, easy preparation, high electrical conductivity as well as corrosion inhibiting behavior. Nevertheless, PPy is insoluble in common solvents and has poor porosity and mechanical properties, limiting its processability in coating [11].

All in all, it is believed that PPy provides corrosion protection for steel [12-13], however to completely understand about the mechanism is still challenging because of different possible oxidation states and experimental parameters. It has been suggested that PPy can reduce the rate corrosion by forming a protective barrier layer and anodic protection, occurring a shift in corrosion potential to more positive values [14]. Due to the balance of charge, negative dopantions such as oxalate, dodecyl sulfate, benzoate anions, cause compensating positive charges to be incorporated into the conjugated pi orbital system. Therefore, counter anions, which present in the backbone of PPy are carried out plays an important role in the doping-dedoping process since it can be released from the polymer during the corrosion reactions [15-16].

In summary, it is noted that the corrosion protection of organic coating is enhanced in the presence of silica/polypyrrole composites. However, the mechanisms of corrosion protection are complex and understanding these mechanisms is complicated by many factors that are likely to influence the processes occurring. In previous study, we investigated that the presence of oxalate anion can significantly enhance the corrosion protection performance of PVB coating. Therefore, this study is focus to understand and highlight the effect of different counter anions to the corrosion performance of silica/polypyrrole composites.

## 2. MATERIALS AND METHODS

### 2.1. Chemicals

Pyrrole (Merck, 97 %) was distilled before use. Tetraethyl orthosilicate (TEOS) was purchased from Daejung, Korea, 98 %; hydrogen chloride (HCl, 36.5 %), Iron (III) chloride hexahydrate ($FeCl_3.6H_2O$, 98 %), sodium oxalate ($Na_2C_2O_4$, 99.5 %), sodium dodecyl sulfate ($C_{12}H_{25}NaO_4S$), sodium benzoate ($C_7H_5NaO_2$, 99 %), acetone ($C_3H_7O$, 99.5 %) and methanol ($CH_4O$, 99.5 %), were purchased from Huakang, China; PVB was purchased from Sekisui, Japan.

### 2.2. Sample preparation

*2.2.1. $SiO_2$/PPyOx composites*

0.15 g of synthesized $SiO_2$ (by sol-gel method, from TEOS and HCl) was dispersed in 0.3 M of an oxidizing agent solution, $FeCl_3$, by using an ultrasonic for 30 minutes. Then one of the three salt solutions: 2.5 mM of sodium oxalate, 2.5 mM of sodium dodecyl sulfate or 2.5 mM of sodium benzoate was added to this mixture and stirred at room temperature for 1 hour and labeled as $SiO_2$/PPyOx, $SiO_2$/PPyODoS and $SiO_2$/PPyBz, respectively. Then 0.01 M of pyrrole was injected slowly in the above mixture for the polymerization of the pyrrole monomer. This process was kept under stirring for 24 hours. Then the synthesized composites were washed with distilled water, and then with a mixture of methanol and acetone (volume ratio 1:1) to remove excess of oxidizing agent. Finally, the synthesized products were dried at 80 $^oC$ for 24 hours in a vacuum oven.

*2.2.2. PVB coatings*

Carbon steel plates (150 mm × 100 mm × 2 mm) were used as substrates. The chemical composition of the steel in weight percent including 0.35 % C, 0.65 % Mn, 0.25 % Si, 0.035 % P and Fe to balance (wt%). The sample surface was abraded with successive SiC papers from 80 to 600 grades and washed with ethanol. The composites were incorporated in PVB coatings at 10 wt.% and dispersed in PVB solution by magnetic stirring followed by an ultrasonic treatment (for 4 hours). The liquid paint was applied by spin coating and dried at ambient temperature for 5 days. The dry film thickness was 11 ± 2 µm (measured by Minitest 600 Erichen digital meter).

**2.3. Analytical methods**

The particle size and morphology of synthesized composites were determined by field emission Scanning Electron Microscope using a Hitachi 4800 machine (SEM).

Thermo gravimetric analyses (TGA) were performed using a TG 209 F1 Libra apparatus (Netzsch), in the range of 25-850 $^oC$, with a heating rate of 10$^oC$ per minute in air.

The FTIR spectra of synthesized composites were obtained using the KBr method KBr pellet technique on a Nicolet IS10 spectrometer operated at 1 $cm^{-1}$ resolution in the range of 400–4000 $cm^{-1}$ region.

The conductivity of synthesized composites was measured by cyclic voltammetry (CV) method through the two-point-electrode without electrolyte on an electrochemical workstation (IM6 Zahner- Elektrik). Samples were prepared in pellet form. The conductivity was calculated by the following equation:

$$\sigma = \frac{\Delta I \times d}{\Delta U \times A} \quad (1)$$

where, σ is the conductivity (S/cm), ΔU is the potential difference (V), ΔI is the resulting current intensity (A), d is thickness of the sample (cm) and A is its area ($cm^2$).

Protection performance of coatings was evaluated by open circuit potential, Tafel polarization and electrochemical impedance measurements using a VMP3-BioLogic Science Instrument. A three-electrode cell was used with a platinum auxiliary electrode, a saturated calomel reference electrode (SCE) and a coated carbon steel working electrode with an exposed area of 11 $cm^2$. Impedance measurements were performed in the 100 kHz–0.01 Hz frequency range at OCP by applying a 10 mV sinusoidal potential signal. The polarization curves were obtained starting from the open circuit potential and varying in the range ±200 mV, with a scan

rate of 5 mV/s. The values of corrosion potential ($E_{corr}$), corrosion current density ($i_{corr}$), anodic and cathodic Tafel constants($\beta_a$, $\beta_c$) obtained by the extrapolation of the linear portions of Tafel plots. The polarization resistance (Rp) values were calculated by using the Stern–Geary equation (2).

$$R_p = \frac{1}{i_{corr}} \times \frac{\beta_a \times \beta_c}{2.303\ (\beta_a + \beta_c)} \quad (2)$$

The corrosive medium was a 3 % NaCl solution. Each experiment was done at least three times.

## 3. RESULTS AND DISCUSSION

### 3.1. Analytical characterization

Figure 1 showed the infrared spectra of $SiO_2$, PPy, $SiO_2$/PPyDoS, $SiO_2$/PPyOx and $SiO_2$/PPyBz. The spectrum of silica shows absorption bands of Si-O-Si antisymmetric and symmetric stretching vibration at 3450 $cm^{-1}$ characteristic of –OH group and peaks at 1080 and 464 $cm^{-1}$ characteristic [17-18].

The spectrum of PPy shows the characteristic bands attributable to the C–H in-plane deformation vibration at 1069 $cm^{-1}$, C–C asymmetric stretching vibration at 1450 $cm^{-1}$, ring-stretching mode of pyrrole ring at 1530 $cm^{-1}$, the peak occurring around 3572-3392 $cm^{-1}$, correspond to the N-H stretch of the pyrrole ring and maybe stretching vibrations of adsorbed water [19].

The spectra of $SiO_2$/PPyBz illustrated a slight shifting of characteristic peaks of silica and polypyrrole and no other peak is observed.

The spectrum of $SiO_2$/PPyDos at 1527 $cm^{-1}$ is associated with C-C stretching vibration and the peak at 1435 $cm^{-1}$ represents C-N stretching vibrations. In addition, the peaks at 1170 $cm^{-1}$ and 1080 $cm^{-1}$ are assigned to S=O stretching vibration of sulfonic acid and Si-O-Si, respectively. In sodium dodecyl sulfate, the corresponding vibration of S=O is at 1176 $cm^{-1}$, the slight different here may be due to the band between PPy and dodecyl sulfate anion [20].

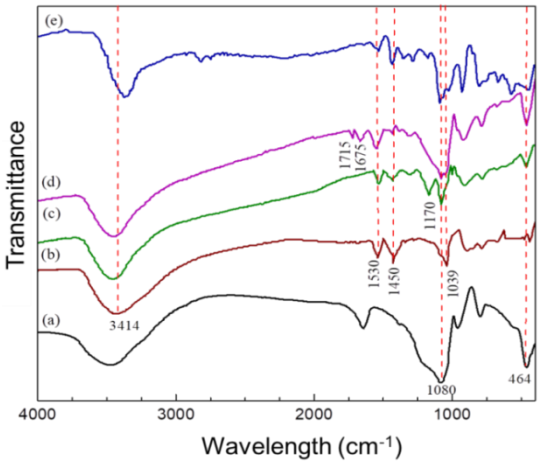


*Figure 1.* FT-IR spectra of $SiO_2$ (a), PPy (b), $SiO_2$/PPyDoS (c), $SiO_2$/PPyOx (d) and $SiO_2$/PPyBz (e).

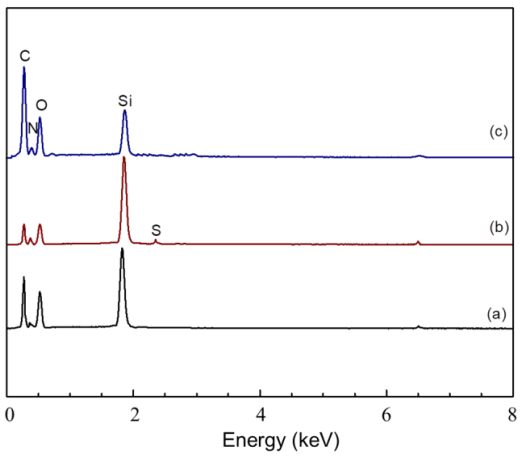


*Figure 2.* EDX of composites $SiO_2$/PPyOx (a), $SiO_2$/PPyDoS (b) and $SiO_2$/PPyBz (c).

With $SiO_2$/PPyOx, there are characteristic bands of PPy and $SiO_2$. The absorption bands at 1530, 1440 and 1075 $cm^{-1}$ are associated with C-C, C-N and Si-O-Si vibrations, respectively. The shifting to lower wavenumbers may be attributed to the interaction between $SiO_2$ and polypyrrole through hydrogen bonding between proton on N-H and oxygen atom on $SiO_2$. Beside this, there are characteristic bands of oxalate anions attributable to C=O stretching vibrations at 1670 and 1710 $cm^{-1}$. The bands at 1440 $cm^{-1}$ may be corresponding to O–C=O stretching vibrations, which is overlapped by the peak of C-N vibration of PPy. These bands appear slightly displaced from the positions of the corresponding vibrations in sodium oxalate (1416 and 1633 $cm^{-1}$) as would be expected for an anion that has been incorporated into composites by the O-H banding [21]. Thus, the FTIR spectra of the composite confirm the incorporation of PPy, $SiO_2$ and counter anions.

*Table 1.* EDX datas of composites $SiO_2$/PPyOx, $SiO_2$/PPyDoS and $SiO_2$/PPyBz.

| Element / Weight % | C | O | N | Si | S |
|---|---|---|---|---|---|
| $SiO_2$/PPyOx | 39.68 | 31.43 | 8.41 | 20.48 | 0.00 |
| $SiO_2$/PPyDoS | 39.73 | 28.94 | 7.05 | 21.19 | 3.19 |
| $SiO_2$/PPyBz | 40.05 | 30.35 | 9.35 | 20.25 | 0.00 |

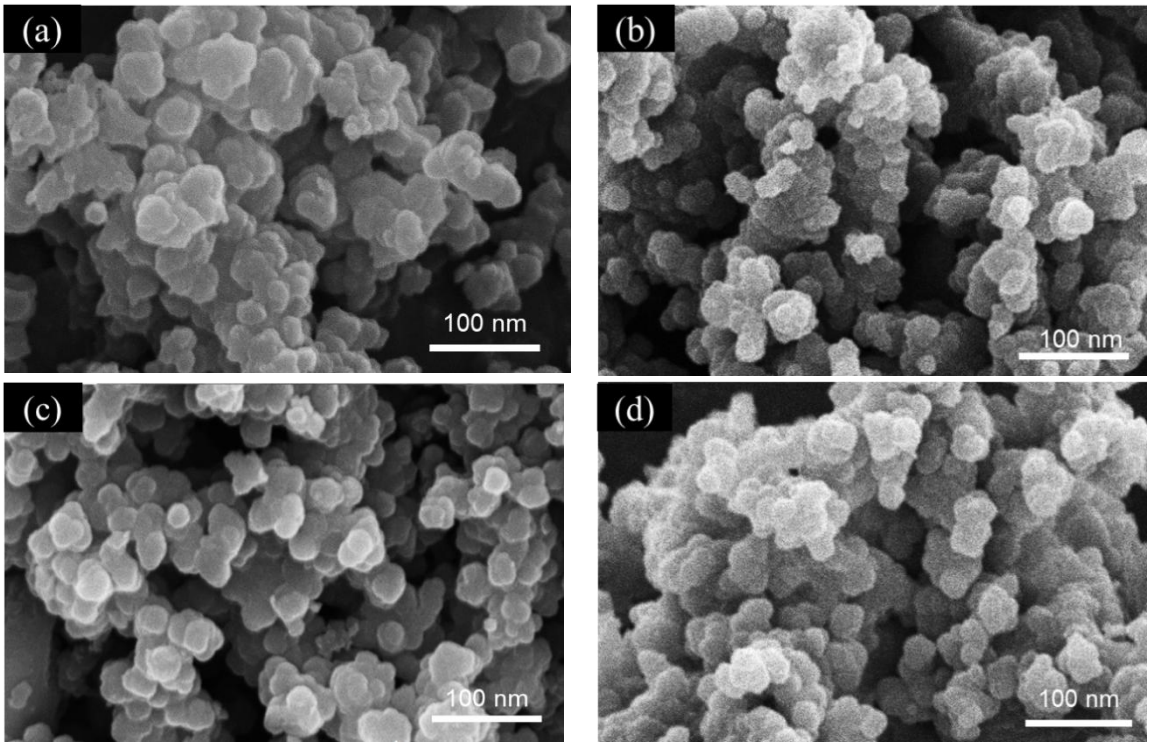


*Figure 3.* SEM images of $SiO_2$/PPy (a), $SiO_2$/PPyDoS (b), $SiO_2$/PPyOx (c) and $SiO_2$/PPyBz (d).

Elemental composition of $SiO_2$/PPyDoS, $SiO_2$/PPyOx and $SiO_2$/PPyBz which are determined by EDX are shown in Figure 2 and Table 1. The results show that composites are

mainly composed of carbon and nitrogen, which are the main elements in the pyrrole compound while oxygen and silicon from silica, sulfur from anion dodecyl sulfate.

Figure 3 a, b, c and d present the SEM images of $SiO_2$/PPy, $SiO_2$/PPyDoS, $SiO_2$/PPyOx and $SiO_2$/PPyBz. The results showed that counter anions does not affect to the morphology of the composites. In the presence of anion dodecyl sulfate, oxalate and benzoat, the synthesized composites are spherical, about 20 to 50 nm.

Figure 4 shows TGA thermograms of composites $SiO_2$/PPy, $SiO_2$/PPyDoS and $SiO_2$/PPyOx. The weight loss occures in four different stages with a total mass loss of $SiO_2$/PPy, $SiO_2$/PPyDoS, $SiO_2$/PPyOx and $SiO_2$/PPyBz are 39 %, 52 %, 58 % and 59 % at 850 $^oC$, respectively. The initial weight loss can be observed at temperatures below 100$^oC$ due to the elimination of absorbed water. The second stage can be observed from 100 to 300$^oC$ due to the breaking of the bond affinity between the PPy and counter anion in the polymers [22].

The major mass loss occurs in the third stage, which takes place at temperatures above 300$^oC$ and occurs until 750 $^oC$. Thereafter, no appreciable changes in weight are observed in the polymer. The total weight loss of $SiO_2$/PPyOx is higher than that of $SiO_2$/PPyDoS, it may be explained as the following way. The decomposition temperature of $SiO_2$ is about 1000 $^oC$ [23] so the higher percentage of silicon in $SiO_2$/PPyDoS, the lower weight loss of nanocomposites, as evidenced by the EDX results. The same strategy can be used to understand the thermal stablity of $SiO_2$/PPyBz, the higher composition of easy decomposition elements such as carbon, oxy, nitro, the higher total weight loss.

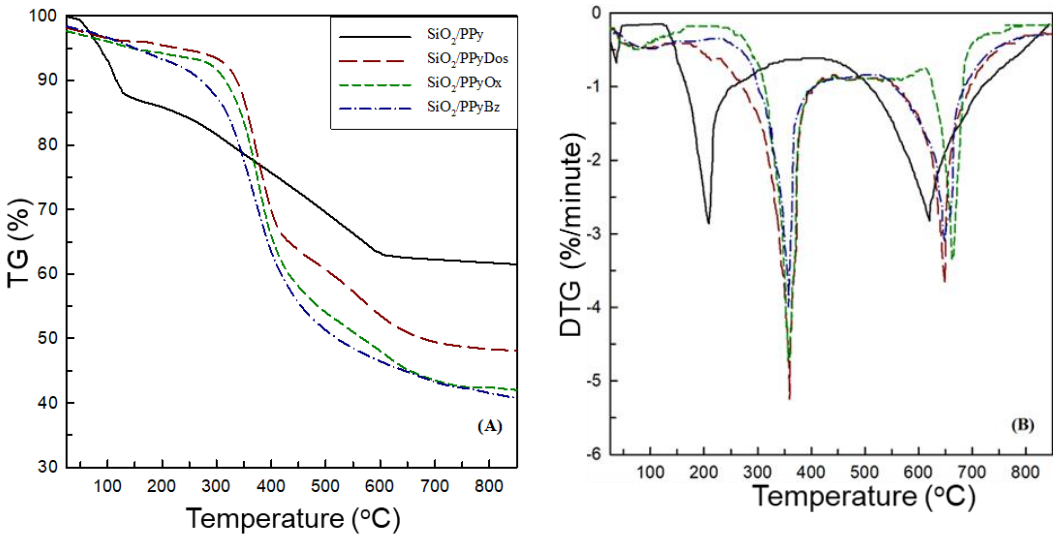


*Figure 4*. TG (A) and DTG (B) diagrams of $SiO_2$/PPy, $SiO_2$/PPyOx, $SiO_2$/PPyBz and $SiO_2$/PPyDoS.

### 3.2. Conductivity

The electrical conductivities of $SiO_2$/PPy, $SiO_2$/PPyOx, $SiO_2$/PPyBz and $SiO_2$/PPyDoS were determined through CV-diagrams from Figure 5. The conductivities of $SiO_2$/PPyOx, $SiO_2$/PPyDoS and $SiO_2$/PPyBz were 0.287, 0.109, 0.101 and 0.105 S/cm, respectively, calculated by equation 1. The decrease of conductivities might be due to the lower weight percentage of PPy in nanocomposites and the insulation of $SiO_2$.

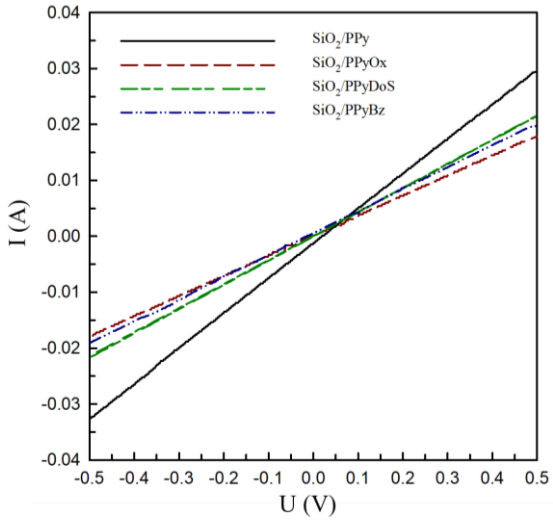


*Figure 5.* CV-diagrams of $SiO_2$/PPy, $SiO_2$/PPyOx, $SiO_2$/PPyDoS and $SiO_2$/PPyBz.

### 3.3. OCP

Figure 6 shows the variation in open circuit potential of steel coated PVB with and without 10 %: $SiO_2$/PPy, $SiO_2$/PPyDoS, $SiO_2$/PPyOx or $SiO_2$/PPyBz after 36 hours immersion in NaCl 3 % solution. After immersion time, OCP of all the coatings tended to decline but in different rate.

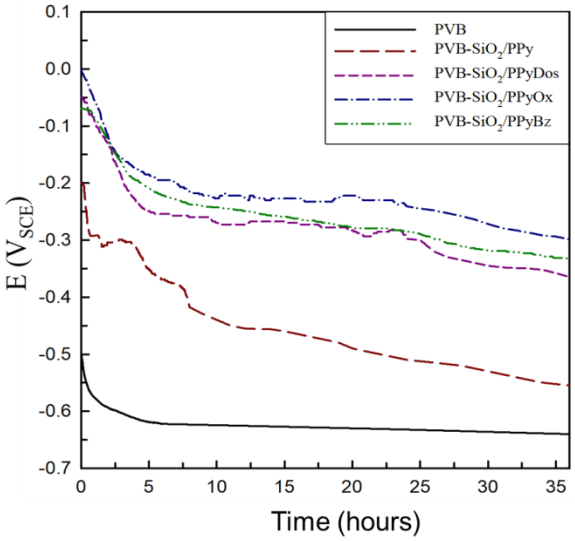


*Figure 6.* Open circuit potential for steel coated PVB and PVB containing 10 %: $SiO_2$/PPy, $SiO_2$/PPyOx, $SiO_2$/PPyBz or $SiO_2$/PPyDoS after 36 immersion hours in 3 % NaCl solution.

At the beginning, the potential of steel coated PVB is lower (-0.55 V) and the potential of steel coated PVB with $SiO_2$/PPy, $SiO_2$/PPyOx, $SiO_2$/PPyBz and $SiO_2$/PPyDoS are higher, -0.25 $V_{SCE}$; -0.002 $V_{SCE}$; -0.07 $V_{SCE}$ and -0.05 $V_{SCE}$, respectively. It indicates that composites can shift the potential into anode areas by forming a passive oxide film. With steel coated PVB containing

$SiO_2$/PPy, the potential decreases continuous after 2 hours, then it remain stable for 10 hours and continue decrease, reach -0.86 $V_{SCE}$ after 36 hours immersion.

The potential of steel coated PVB containing $SiO_2$/PPyOx decreases after hours immersion, reach -0.12 $V_{SCE}$. In the case of $SiO_2$/PPyDoS and $SiO_2$/PPyBz, those values decline after 5 immersion hours, attain -0.25 $V_{SCE}$ and -0.22 $V_{SCE}$, respectively. That may be due to the uptaking of chloride ions to the coatings. But after that, the potential is remains stable for 22 and 19 hours with $SiO_2$/PPyOx and $SiO_2$/PPyDoS, $SiO_2$/PPyBz respectively. It emphasizes that coated steel samples are still in the passive state because of the reduction of PPy and releasing of counter anions, simultaneously. This shows that coatings have exhibited effective barrier behavior and limited the motion of corrosive agent towards the underlying steel. After that, the potentials of steel coated with PVB-$SiO_2$/PPyOx, PVB-$SiO_2$/PPyBz and PVB-$SiO_2$/PPyDoS continue decrease, reach -0.3 $V_{SCE}$, -0.33 $V_{SCE}$ and -0.365 $V_{SCE}$ after 36 exposure hours, respectively. These results indicated that $SiO_2$/PPyOx shows the best corrosion inhibitor ability.

### 3.4. Tafels polarization curves

Figure 7 show Tafels polarization curves for steel coated with PVB and PVB containing 10 % $SiO_2$/PPy, $SiO_2$/PPyOx, $SiO_2$/PPyDoS and $SiO_2$/PPyBz after 24 hours immersion in 3 % NaCl solution. The values of corrosion potential ($E_{corr}$), corrosioncurrent density ($i_{corr}$), anodic and cathodic Tafel constants ($\beta_a$, $\beta_c$), polarization resistance (Rp) are given in Table 2.

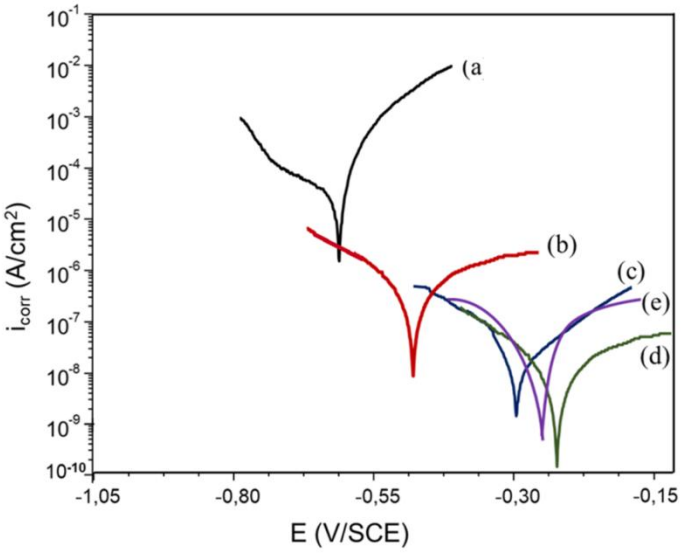


*Figure 7.* Tafel plots of steel coated with PVB (a), PVB containing 10% of: $SiO_2$/PPy (b), $SiO_2$/PPyDoS (c), $SiO_2$/PPyOx (d) or $SiO_2$/PPyBz (e) in 3% NaCl solution after 24 hours immersion.

The occurrence of notably higher value of anodic and cathodic Tafel constants for PVB coatings with nanocomposites implies the effective role of nanocomposites in cotrolling anodic and cathodic corrosion reactions. Futher, compared with steel coated with PVB (-0.611 $V_{SCE}$), the corrosion potential for steel coated with PVB-$SiO_2$/PPy, PVB-$SiO_2$/PPyDoS and PVB-$SiO_2$/PPyOx shift to more positive regions (-0.482 $V_{SCE}$, -0.298 $V_{SCE}$, -0.254 $V_{SCE}$ and -0.242 $V_{SCE}$, respectively) after 24 hours immersion. In addition, the corrosion current density decrease, in ordered: steel coated with PVB ($2.78\times10^{-4}$ A.cm$^{-2}$) > steel coated with PVB-$SiO_2$/PPy

($8.25\times10^{-7}$ A.cm$^{-2}$) > steel coated with PVB-$SiO_2$/PPyDoS ($1.02\times10^{-7}$ A.cm$^{-2}$) > steel coated with PVB-$SiO_2$/PPyBz ($4.32\times10^{-7}$ A.cm$^{-2}$) > steel coated with PVB-$SiO_2$/PPyOx ($4.81\times10^{-8}$ A.cm$^{-2}$). On the contrary, the polarization resistance values of samples are followed the opposite order. These results indicated that composites of $SiO_2$/PPyDoS, $SiO_2$/PPyBz and $SiO_2$/PPyOx play an important role and $SiO_2$/PPyOx composite shows the best corrosion protection performance.

*Table 2*. $E_{corr}$, $i_{corr}$, $\beta_a$, $\beta_c$and $R_p$ values of the steel coated with PVB, PVB containing 10 % $SiO_2$/PPy, $SiO_2$/PPyDoS, $SiO_2$/PPyOx and $SiO_2$/PpyBz after 24 hours immersion in 3 % NaCl solution.

| Samples | $E_{corr}$ (V/SCE) | $\beta_a$ (V dec$^{-1}$) | $-\beta_c$ (V dec$^{-1}$) | $i_{corr}$ (A.cm$^{-2}$) | $R_p$ (Ω) |
|---|---|---|---|---|---|
| **PVB** | -0.611 ± 0.002 | 0.314 ± 0.001 | 0.305 ± 0.001 | $2.78\times10^{-4}$ ± $1\times10^{-5}$ | $2.41\times10^{2}$ ± 1 |
| **PVB-$SiO_2$/PPy** | -0.482 ± 0.003 | 0.332 ± 0.001 | 0.309 ± 0.001 | $8.25\times10^{-7}$ ± $5\times10^{-9}$ | $8.4\times10^{4}$ ± 5 |
| **PVB-$SiO_2$/PPyDoS** | -0.298 ± 0.001 | 0.356 ± 0.001 | 0.311 ± 0.001 | $1.02\times10^{-7}$ ± $3\times10^{-9}$ | $7.1\times10^{5}$ ± 8 |
| **PVB- $SiO_2$/PPyBz** | -0.254 ± 0.001 | 0.358 ± 0.001 | 0.327 ± 0.001 | $9.03\times10^{-8}$ ± $5\times10^{-10}$ | $8.2\times10^{5}$ ± 10 |
| **PVB- SiO2/PPyOx** | -0.242 ± 0.001 | 0.378 ± 0.001 | 0.396 ± 0.001 | $4.81\times10^{-8}$ ± $4\times10^{-10}$ | $1.7\times10^{6}$ ± 10 |

### 3.5. EIS

Bode graphs of PVB, PVB containing 10 % $SiO_2$/PPy, $SiO_2$/PPyBz, $SiO_2$/PPyDoS coatings after 1 hour exposure in 3 % NaCl solution are shown in Figure 8. Impedance module of coating containing composite showed the higher value than that of coating without composite. More interesting, phase plots of all coatings show only one time constant supporting the reaction on the coating surface.

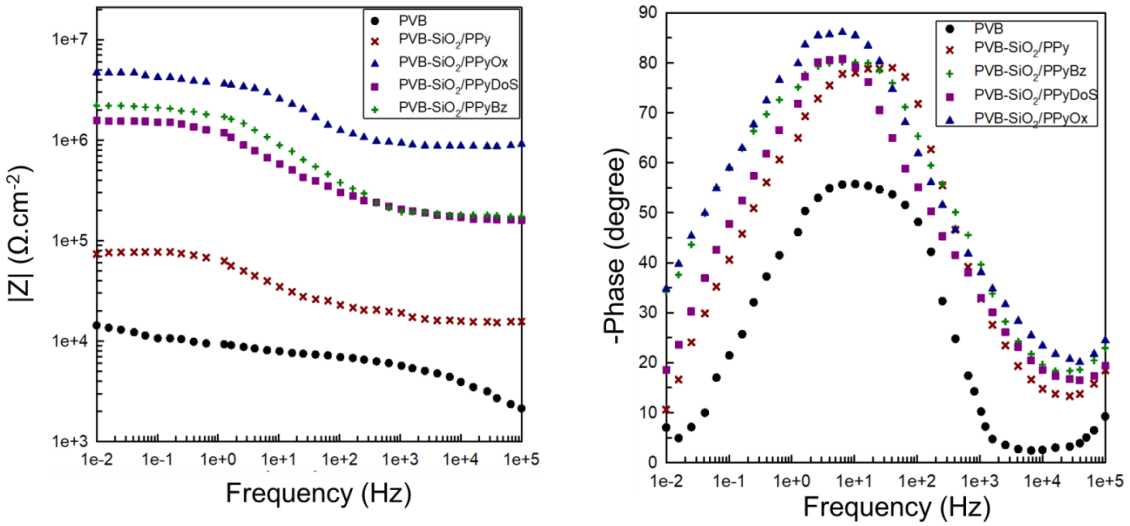


*Figure 8.* Bode plots of steel coated with PVB and PVB containing composites after 1 hour immersion.

In the low frequencies zone from 0.01 Hz to 1 Hz, impedance module value of steel coated with PVB- $SiO_2$/PPy is 8 times higher than that of steel coated with PVB. At 1 Hz, impedance modulus of PVB-$SiO_2$/PPyBz, PVB-$SiO_2$/PPyDoS and PVB-$SiO_2$/PPyOx attain $1.71\times10^6$, $1.19\times10^6$ and $3.64\times10^6$ $\Omega.cm^{-2}$, respectively, about 30 times higher than that of PVB-$SiO_2$/PPy ($6.28\times10^4$ $\Omega.cm^{-2}$). The impedance module in low frequency zone is presented for the corrosion reactions at the interface between coating and steel, the high values in this zone indicated the presence of counter anions can enhance the corrosion protection behavior of PVB coating. These results indicated that after 1 hour exposure, the steel surface is protected from the corrosive ions in solution.

After 24 hours of immersion (Figure 9), it is clear to observe the decrease of protection ability of PVB coating with steel, impedance module graph shows the same trend with uncoated steel. With the presence of composites, these values also reduce but always higher than that of samples without composites. These results are confirmed by the phase diagram, with the appearance of two time constants with PVB, PVB-$SiO_2$/PPy, $SiO_2$/PPyDoS and PVB-$SiO_2$/PPyBz, supporting the diffusion of corrosive agent towards the underlying steel. On the other hand, with PVB-$SiO_2$/PPyOx, only one time constants is observed and the maximal phase angle values are high in a wide frequency range, showing the protective properties of coating. However, at 10 mHz, impedance values decrease to $3.34\times10^4$, $3.34\times10^4$ and $4.27\times10^4$ $\Omega.cm^{-2}$ with PVB-$SiO_2$/PPyDoS, PVB-$SiO_2$/PPyBz and PVB-$SiO_2$/PPyOx, respectively.

These obtained results confirm that oxalate anion offers more effective protection which may be due to its size. Polypyrrole with small incorporated counter anions as oxalate exhibits anion exchange behavior due the high mobility of anion in its matrix. Then corrosive agent such as chloride anion is trapped in the polymer matrix thus the steel surface is protected. When oxalate anions are released, it can incorporate with ferric cations to form ferric oxalate complex, a second passive layer.

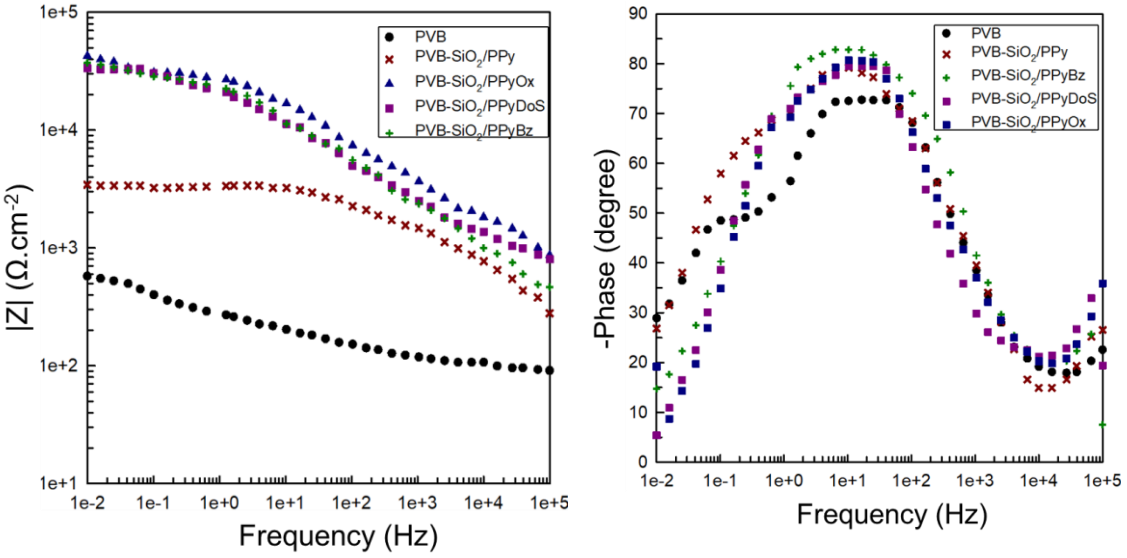


*Figure 9.* Bode plots of steel coated with PVB and PVB containing composites after 24 hours immersion.

Impedance modulus at low frequency $|Z_{100mHz}|$ is an important factor to evaluate corrosion resistant properties of coatings. Figure 10 shows the $|Z_{100mHz}|$ of different coatings on steel after immersion times in 3 % NaCl solution. The $|Z_{100mHz}|$ values follow the order: PVB < PVB-

$SiO_2$/PPy < PVB-$SiO_2$/PPyDoS < PVB-$SiO_2$/PPyBz < PVB-$SiO_2$/PPyOx. It proves that the existence of counter anions can improve the anticorrosion performance of PVB coatings.

EIS data suggest that PVB-$SiO_2$/PPyOx coating should have better corrosion resistant properties than PVB-$SiO_2$/PPyDoS and PVB-$SiO_2$/PPyBz coating due to its much higher impedance values, in particular at the low frequency. Therefore, the EIS results are in agreement with the results obtained by open circuit potential.

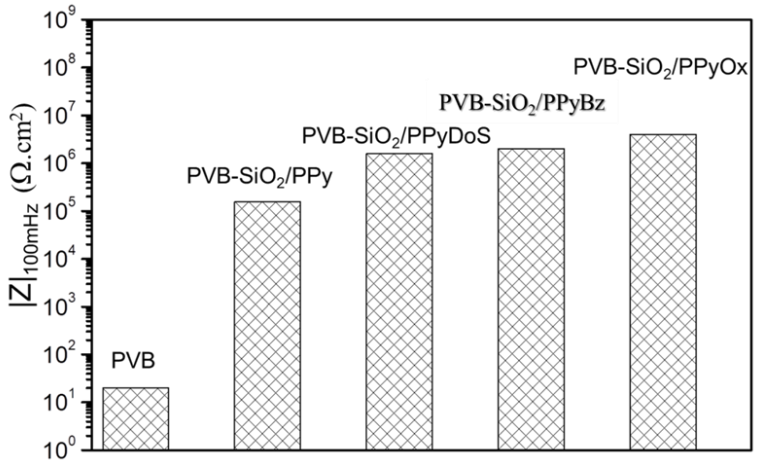


*Figure 10.* $|Z_{100mHz}|$ of steel coated with PVB and PVB containing composites after 24 hours immersion.

## 4. CONCLUSIONS

The protection performance of PVB coating containing silica/polypyrrole composites with different counter anions (dodecyl sulfate, oxalate and benzoate) was investigated by electrochemical characterizations. It was shown that the presence of counter anion significantly enhanced the effect of $SiO_2$/PPy on protection performance of PVB coatings for carbon steel, especially oxalate anion, by dual mechanism by forming a passivating layer as well as increasing physical barrier ability. These results reveal that the silica/polypyrrol-oxalate composite has good corrosion protection properties and it can be considered as a potential inhibitor for PVB coating for the corrosion protection of carbon steel in 3 % NaCl solution.

***Acknowledgements.*** The research funding from Vietnam National Foundation for Science and Technology Development (NAFOSTED) (Grant number: 104.06-2014.12) was acknowledged.

## REFERENCES

1. Bowman E. - International Measures of Prevention, Application and Economics of Corrosion Technologies Study, NACE international **1** (2016) 1-20.
2. Tian Z., Yu H., Wang L., Saleem M., Ren F., Sun R., Sun Y. and Huang L. - Recent progress in the preparation of polyaniline nanostructures and their applications in anticorrosive coatings, Royal Society of Chemistry Advances **4** (2014) 28195-28208.
3. Niratiwongkorn T., Luckachan G. E. and Mittal V. - Self-healing protective coating of polyvinyl butyral/polypyrrole-carbon black composite on carbon steel, Royal Society of Chemistry Advances **6** (2016) 43237-43249.

4. Radhakrishnan S., Siju S. R., Mahanta D., Patil S. and Madras G. - Conducting polyaniline–nano-$TiO_2$ composites for smart corrosion resistant coatings, Electrochimica Acta **54** (2009) 1249-1254.
5. Bakhshandeh E., ZahraRanjbar A., Sobhani S. and RezaSaeb M. - Anti-corrosion hybrid coatings based on epoxy–silica nano-composites: Toward relationship between the morphology and EIS data, Progress in Organic Coatings **77** (7) (2014) 1169-1183.
6. Jalili M. M. and Moradian S. - Deterministic performance parameters for an automotive polyurethane clearcoat loaded with hydrophilic or hydrophobic nano-silica, Progress in Organic Coatings **66** (4) (2009) 359-366.
7. Rupali G. and Amitabha D. - Conducting Polymer Nanocomposites: A Brief Overview, Chemistry of Materials **12** (2000) 608-622.
8. Heeger A.J. - Semiconducting and Mettalic Polymers, (Nobel Lecture) The fourth generation of Polymeric Materials, Angewandte Chemie **40** (14) (2001) 2591-2611.
9. MacDiarmid, A.G. - Synthetic Metals, a novel role for organic polymers, (Nobel Lecture), Angewandte Chemie **40** (14) (2001) 2581-2590.
10. Shirakawa H. - The discovery of Polyacetylene Film: The Dawning of an Era of Conductive Polymers, (Nobel Lecture), Angewandte Chemie **40** (14) (2001) 2574-2580.
11. Yan M., Vetter C. A. and Gelling V. J. - Corrosion inhibition performance of polypyrrole Al flake composite coatings for Al alloys, Corrosion Science **70 (**2013) 37-45.
12. Qi K., Qiu Y., Chen Z. and Guo X. - Corrosion of conductive polypyrrole: Galvanic interactions between polypyrrole and metal substrates, Corrosion Science **91** (2015) 272-280.
13. Van V. T. H., Hang T. T. X., Nam P. T., Phuong N. T., Thom N. T., Devilliers D. and Thanh D. T. M. - Synthesis of silica/polypyrrole nanocomposites and application in corrosion protection of carbon steel, Journal of Nanoscience and Nanotechnology **18** (2018) 4189-4195.
14. Beck F., Michaelis R., Schloten F. and Zinger B. - Filmforming electropolymerization of pyrrole on iron in aqueous oxalic acid, Electrochimica Acta **39** (1994) 229-234.
15. Iroh J. O. and Su W. - Corrosion performance of polypyrrole coating applied to low carbon steel by an electrochemical process," Electrochimica Acta **46** (2000) 15-24.
16. Duc L. M. Trung V. Q. - Layers of Inhibitor Anion – Doped Polypyrrole for Corrosion Protection of Mild Steel, Materials Science, IntechOpen **7** (2013) 143-174.
17. Yang F., Chu Y., Ma S., Zhang Y. and Liu J. - Preparation of uniform silica/polypyrrole core/shell microspheres and polypyrrole hollow microspheres by the template of modified silica particles using different modified agents, Journal of Colloid and Interface Science **301** (2006) 470–478.
18. Kim Y. D. and Hong G. - Electrorheological properties of polypyrrole-silica nanocomposite suspensions, Korean Journal Chemistry English **29** (7) (2012) 964-968.
19. Jeon I. Y., Choi H. J., Tan L. S., Baek J. B. - Nanocomposite prepared from in situ grafting of polypyrrole toaminobenzoyl-functionalized multiwalled carbon nanotube and its electrochemical properties, Journal of Polymer Science Part A: Polymer Chemistry **4** (2011) 2529–2537.

20. Mohammadi A., Yamini Y. and Alizadeh N. - Dodecylsulfate-doped polypyrrole film prepared by electrochemical fiber coating technique for headspace solid-phase microextraction of polycyclic aromatic hydrocarbons, Journal of Chromatography A **1063** (1-2) (2005) 1-8.
21. Miller E. T., Benally K. J., GreyEyes S. D. and McKenzie J. T. – Determination of oxalate ion dopant level in polypyrrole using FT-IR, Journal of Undergraduate Chemistry Research **13** (1) (2014) 5-8.
22. Wei Y. and Hsueh K. F. - Thermal analysis of chemically synthesized polyaniline and effects of thermal aging on conductivity, Journal of Polymer Science **27** (13) (1989) 4351-4363.
23. Vansant. E. F., Voort. P. V. D. and Vrancken K. C. - Characterization and Chemical Modification of the Silica Surface, Studies in Surface Science and Catalysis, Elsevier **93** (1995) 3-556.